JBC Papers in Press. Published on December 20, 2002 as Manuscript M211682200

Epac-Selective cAMP Analog 8-pCPT-2'-O-Me-cAMP As A Stimulus For Ca^{2+}-Induced Ca^{2+} Release And Exocytosis In Pancreatic β-Cells

Running Title: cAMP, Epac and CICR in pancreatic β-Cells

Guoxin Kang[1], Jamie W. Joseph[2], Oleg G. Chepurny[1], Marie Monaco[1], Michael B. Wheeler[2], Johannes L. Bos[3], Frank Schwede[4], Hans-G. Genieser[4] and George G. Holz[1,5]

[1] Department of Physiology and Neuroscience
New York University School of Medicine
New York, NY, 10016 USA

[2]Departments of Physiology and Medicine
University of Toronto
Toronto, Canada

[3]Department of Physiological Chemistry And Centre for Biomedical Genetics
University Medical Center Utrecht
Universiteitsweg 100
3584CG Utrecht
The Netherlands

[4]BIOLOG Life Science Institute
P.O. Box 107125
D-28071 Bremen, Germany

[5] Corresponding Author:
G.G. Holz, Ph.D.
Associate Professor
Department of Physiology and Neuroscience
New York University School of Medicine
New York, NY 10016
Tel. 212-263-5434
Fax 212-689-9060
Email: holzg01@popmail.med.nyu.edu

SUMMARY

The second messenger cAMP exerts powerful stimulatory effects on Ca^{2+} signaling and insulin secretion in pancreatic β-cells. Previous studies of β-cells focused on protein kinase A (PKA) as a down stream effector of cAMP action. However, it is now apparent that cAMP also exerts its effects by binding to cAMP-regulated guanine nucleotide exchange factors (Epac). Although one effector of Epac is the Ras-related G protein Rap1, it is not fully understood what the functional consequences of Epac-mediated signal transduction are at the cellular level. 8-(4-chloro-phenylthio)-2'-*O*-methyladenosine-3'-5'-cyclic monophosphate (8-pCPT-2'-O-Me-cAMP) is a newly described cAMP analog, and it activates Epac, but not PKA. Here we demonstrate that 8-pCPT-2'-O-Me-cAMP acts in human pancreatic β-cells and INS-1 insulin-secreting cells to mobilize Ca^{2+} from intracellular Ca^{2+} stores *via* Epac-mediated Ca^{2+}-induced Ca^{2+} release (CICR). The cAMP-dependent increase of $[Ca^{2+}]_i$ that accompanies CICR is shown to be coupled to exocytosis. We propose that the interaction of cAMP and Epac to trigger CICR explains, at least in part, the blood glucose-lowering properties of an insulinotropic hormone (glucagon-like peptide-1, also known as GLP-1) now under investigation for use in the treatment of type-2 diabetes mellitus.

INTRODUCTION

cAMP-regulated guanine nucleotide exchange factors (referred to here as Epac) link cAMP production to the activation of the Ras-related small molecular weight G protein Rap1 (1,2). Two isoforms of Epac have been described (Epac1, Epac2) (1,2), and each is proposed to mediate the PKA-independent signal transduction properties of cAMP. Analysis of cAMP-mediated signaling pathways is complicated by the lack of specificity with which cAMP acts. cAMP targets not only PKA and Epac, but also certain cAMP phosphodiesterases and ion channels (3). Recent structure-function analyses of cAMP action demonstrate that introduction of a 2'-methoxy group in place of the 2'-hydroxyl group of cAMP confers Epac specificity to the cyclic nucleotide (4). One such analog is 8-(4-chloro-phenylthio)-2'-*O*-methyladenosine (8-pCPT-2'-O-Me-cAMP). Rap1 activation assays conducted *in vitro* demonstrate that 8-pCPT-2'-O-Me-cAMP binds to and activates Epac1 with higher apparent affinity (EC_{50} 2.2 μM) than cAMP itself (EC_{50} 30 μM) (4). Furthermore, 8-pCPT-2'-O-Me-cAMP is a weak activator of PKA (4). To date, the properties of 8-pCPT-2'-O-Me-cAMP in living cells have been evaluated only with respect to its ability to promote Epac-mediated activation of Rap1 (4). We now demonstrate that 8-pCPT-2'-O-Me-cAMP is an effective stimulus for Ca^{2+}-induced Ca^{2+} release (CICR) and exocytosis in human pancreatic β-cells and an insulin-secreting cell line (INS-1). The action of 8-pCPT-2'-O-Me-cAMP is shown to be independent of PKA, but is blocked by over expression of dominant negative Epac2. Therefore, 8-pCPT-2'-O-Me-cAMP is likely to serve as a specific pharmacological tool for analyses of PKA-independent signaling properties of cAMP in the regulation of intracellular Ca^{2+} signaling and exocytosis.

EXPERIMENTAL PROCEDURES

Cell culture- Human islets of Langerhans were provided under the auspices of the Juvenile Diabetes Research Foundation International Islet Distribution Program. Single cell suspensions of human islet cells were prepared by digestion with Trypsin-EDTA, and the cells were plated onto glass coverslips (25CIR-1; Fisher Sci.) coated with 1 mg/ml concanavalin A (type V; Sigma Chem. Co., St. Louis, MO). Cell cultures were maintained in a humidified incubator (95% air, 5% CO_2) at 37 ^{o}C in CMRL-1066 culture medium containing 10% fetal bovine serum (FBS), 100 U/ml penicillin G, 100 µg/ml streptomycin, and 2.0 mM L-glutamine. INS-1 cells (passages 70–90) were maintained in RPMI 1640 culture medium containing 10 mM HEPES, 11.1 mM glucose, 10% FBS, 100 U/ml penicillin G, 100 µg/ml streptomycin, 2.0 mM L-glutamine, 1.0 mM sodium pyruvate, and 50 µM 2-mercaptoethanol (5). INS-1 cells were passaged by trypsinization and subcultured once a week. All reagents for cell culture were obtained from Invitrogen LifeTechnologies (Rockville, MD).

Plasmid and adenovirus constructs- A plasmid in which expression of enhanced yellow fluorescent protein (EYFP) was placed under the control of the rat insulin II gene promoter (RIP2) was constructed by fusing a -695 bp BamH1 fragment of RIP2 to the coding sequence of EYFP contained within the pEYFP-N1 expression plasmid (Clonetech, Palo Alto, CA). Lipofectamine Plus reagent (Invitrogen Life Technologies) was used to transfect INS-1 cells with this plasmid designated as RIP2-EYFP, and clones of INS-1 cells exhibiting stable transfection were obtained by antibiotic resistance selection using G418. For construction of adenovirus, RIP2-EYFP was PCR amplified inserting XhoI (5' end, primer CTC GAG ACC GCG GGC CCG GGA TCC) and KpnI (3' end, primer GGT ACC CCT CTA CAA ATG TGG TAT GGC TG) digestion sites on either end of the RIP2-EYFP sequence. The PCR product was subcloned into pCR2.1 and RIP2-EYFP was then inserted into a XhoI/ KpnI site of AdLox.HTM. The RIP2-EYFP-AdLox.HTM vector was co-

transfected with psi5 vector into CRE8 cells expressing CRE recombinase. This resulted in recombination of the RIPYFP-AdLox.HTM vector with the psi5 vector (6). The psi5 vector acts as a donor virus to supply viral backbone. AdRIPYFP viral particles generated in this manner were passaged 3 times in CRE8 cells and CsCl gradient purified. 10^9 viral particles/ml were used to infect β-cells or islets.

Immunocytochemistry- Pancreatic islets isolated from male Wistar rats (250 g) were plated on rat tail collagen and infected for 48 hr with AdRIP2EYFP. Islets were stained for insulin using guinea pig anti-insulin and a secondary anti-guinea pig IgG conjugated with Rhodamine TRITC (Jackson immunoresearch laboratories, West Grove, PA). Islets were stained for glucagon using rabbit anti-glucagon, 08-0064, (Zymed, San Francisco, CA) and a secondary anti-rabbit IgG conjugated with Rhodamine TRITC. Laser scanning confocal microscopy was performed (Carl Zeiss, LSM 410, Germany), and images were obtained using a 63X oil immersion objective.

Co-detection of EYFP and fura-2- Expression of EYFP was detected through use of an upright microscope (Eclipse TE300, Nikon Instruments, Melville, NY) equipped with a 75 Watt xenon arc lamp serving as a light source. A liquid light guide directed unfiltered excitation light to an EYFP filter set mounted in a filter cube containing an HQ500/20 excitation filter, a Q515LP dichroic beamsplitter, and an HQ535/30 emission filter (HQ filter set 41028, Chroma Tech. Corp., Brattleboro, VT). Once an EYFP-positive cell was identified, the filter cube was switched manually to a second filter cube containing components of the fura-2 filter set. Excitation light provided by the xenon arc lamp was reflected by a rotating chopper mirror through 340/20BP and 380/20BP excitation filters (Chroma) mounted in a motorized filter wheel located at the light source. The filtered light was then directed to the fura-2 filter set by way of the liquid light guide. The fura-2 filter cube contained a 400DCLP dichroic beamsplitter and a 510/80 excitation filter (Chroma).

Measurement of $[Ca^{2+}]_i$ - The fura-2 loading solution consisted of a standard extracellular saline (SES) containing (in mM): 138 NaCl, 5.6 KCl, 2.6 $CaCl_2$, 1.2 $MgCl_2$, 10 mM HEPES, and 5.6 mM D-glucose. The SES was supplemented with 1 μM fura-2 acetoxymethyl ester (fura-2 AM; Molecular Probes Inc., Eugene, OR), 2% FBS, and 0.02% Pluronic F-127 (w/v; Molecular Probes Inc.). Cells were exposed to fura-2 AM for 20-30 min at 22 ^{o} C. The loading solution was removed, and cells were washed and equilibrated in fresh SES for 10 min at 22 ^{o} C. Images were acquired using a 100X UVF oil immersion objective (N.A. 1.3, Nikon), and dual excitation wavelength microfluorimetry was performed ratiometrically at 0.5 s intervals using a digital video imaging system outfitted with an intensified CCD camera (IonOptix Corp., Milton, MA). $[Ca^{2+}]_i$ was calculated according to the method of Grynkiewicz and co-workers (7,8). In vitro calibration of raw fluorescence values was performed using fura-2 $(K^+)_5$ salt dissolved in calibration buffers from Molecular Probes Inc. (Calcium Calibration Kit 1 with Mg^{2+}). Values of R_{min} and R_{max} were 0.20 and 7.70.

Electrochemical detection of exocytosis- Cells were loaded with serotonin (5-HT) by incubation in culture medium containing 0.6 mM 5-HT and 0.6 mM 5-hydroxytryptophan. 5-HT is sequestered in large dense-core secretory granules by active transport, but it is excluded from the small synaptic vesicle-like structures that do not contain insulin (9). The release of 5-HT serves as a surrogate marker for insulin secretion (10). Prolonged exposure of β-cells to high concentrations of 5-HT produces toxic effects (11). Therefore, exposure to 5-HT was limited to 4-16 hr. Carbon fiber electrodes for amperometric detection of secreted 5-HT were prepared as described previously (12). A +650 mV potential was applied to a 10 μM diameter carbon fiber, the tip of which was placed adjacent to the cell of interest. The distance from the electrode tip to the cell was approximately 1 μm. An HEKA EPC-9 patch clamp amplifier was used for detection of the amperometric current resulting from oxidation of 5-HT. The signal was filtered at 200

Hz, sampled at 1 kHz, and stored on a MacIntosh G3 computer running PULSE 8.31 software (Heka, Lambrecht, Germany).

Luciferase assay- The activity of CRE-Luc was assessed in lysates of INS-1 cells by use of a luciferase assay as described previously (13-15). After a 4 hr exposure to test substances, cells were lysed and assayed for luciferase-catalyzed photoemissions using a luciferase assay kit (Tropix, Bedford, MA) and a luminometer allowing automated application of ATP and luciferin solutions (Model TR-717, Perkin Elmer Applied Biosystems, Foster City, CA). Experiments were carried out in triplicate. Statistical analyses were performed using the ANOVA test combined with Fisher's PLSD test.

Measurement of inositol phosphate accumulation- INS-1 cells were plated in complete growth medium in 12-well plastic culture dishes. ^{3}H-inositol (10μCi/ml) was added to each well and the cells were incubated for 48 hr. The medium was then changed to serum-free RPMI 1640 containing 10 mM lithium chloride and the pharmacological agents to be tested. The incubation was continued for an additional 60 min at 37 ^{o} C. Cellular lipids and inositol phosphates were extracted for Dowex chromatography and quantification as described previously (16).

Sources of reagents- 8-pCPT-2'-O-Me-cAMP, 8-CPT-cAMP, and Rp-8-Br-cAMPS were obtained from BIOLOG Life Sci. Inst., Germany. GLP-1, Ex-4, acetylcholine, forskolin, 8-Br-cAMP, H-89, KT 5720, and ryanodine were from Sigma Chem. Co. Wild type and dominant negative pSRα plasmids for transfection and the expression of recombinant mouse Epac2 were obtained from the laboratory of Dr. S. Seino (17).

RESULTS

EYFP-based phenotype selection of β-cells- Methodology was developed allowing phenotype selection of β-cells in primary cultures of dispersed islets bathed in standard extracellular saline (SES) containing 7.5 mM glucose. A -695 bp fragment of the rat insulin II gene promoter (RIP2) was fused to the coding sequence of EYFP (18) for initial expression of EYFP in INS-1 cells (Fig.1*A,B*). RIP2-EYFP was then incorporated into an adenoviral vector, and expression of EYFP was conferred to human β-cells by adenovirus-mediated gene transfer using AdRIP2EYFP (Fig.1*C,D*). Confocal microscopy in combination with fluorescence immunocytochemistry demonstrated that expression of EYFP was restricted to the insulin-immunoreactive β-cells and not the glucagon-reactive α-cells in whole islets of Langerhans derived from rat (Fig.2). Functional studies of small clusters of human islet cells demonstrated that only the EYFP-positive β-cells exhibited an increase of $[Ca^{2+}]_i$ when exposed to the insulin secretagogue glyburide (Fig.3).

8-pCPT-2'-O-Me-cAMP as a stimulus for Ca^{2+} signaling in human β-cells- The Epac-selective cAMP analog 8-pCPT-2'-O-Me-cAMP was a highly effective stimulus for Ca^{2+} signaling in human β-cells. Human islet cells infected with AdRIP2EYFP were loaded with fura-2 and EYFP-positive β-cells were identified using the EYFP filter set. Next, the filter set was manually switched to a fura-2 filter set, thereby allowing ratiometric measurements of $[Ca^{2+}]_i$ imaged using an intensified CCD camera. The responsiveness of an EYFP-positive β-cell was demonstrated by measuring the increase of $[Ca^{2+}]_i$ that accompanied a 10 s application of 50 μM 8-pCPT-2'-O-Me-cAMP delivered via a micropipette (Fig.4 *A1,A2*). The phenotype of this cell was additionally confirmed by demonstrating its responsiveness to the insulin secretagogue glyburide (Fig.4 *A2*). The increase of $[Ca^{2+}]_i$ measured in response to 8-pCPT-2'-O-Me-cAMP was blocked by pretreatment of human β-cells with ryanodine (Fig.4*B*).

8-pCPT-2'-O-Me-cAMP as a stimulus for exocytosis in human β-cells- The increase of $[Ca^{2+}]_i$ measured during exposure of 5-HT-loaded human β-cells to 8-pCPT-2'-O-Me-cAMP was associated with exocytosis, as measured by carbon fiber amperometry (Fig.5). The increase of $[Ca^{2+}]_i$ (Fig.5 *A1*) was time-locked to the appearance of amperometric current spikes resulting from the oxidation of released 5-HT (Fig.5 *A2*). When viewed on an expanded time scale, the quantal nature of the individual secretory events was revealed (Fig.5 *A3,A4*). No secretory events were detected in the absence of an increase of $[Ca^{2+}]_i$.

8-pCPT-2'-O-Me-cAMP as a stimulus for CICR in INS-1 cells- The action of 8-pCPT-2'-O-Me-cAMP was also evaluated in the INS-1 insulin-secreting cell line (5). These cells exhibit Epac-mediated CICR manifest as a transient increase of $[Ca^{2+}]_i$ (18). 8-pCPT-2'-O-Me-cAMP was a stimulus for CICR in INS-1 cells (Fig.6*A*), and the kinetics of the increase of $[Ca^{2+}]_i$ matched closely that observed in human β-cells (c.f., Fig.4). The action of 8-pCPT-2'-O-Me-cAMP was mimicked by forskolin (Fig.6*B*) and by 8-Br-cAMP (Fig.6*C*). In some cells, the fast transient increase of $[Ca^{2+}]_i$ was followed by a more slowly developing and sustained increase of $[Ca^{2+}]_i$ (Fig.6*D*). Neither effect of 8-pCPT-2'-O-Me-cAMP was blocked by the cAMP antagonist Rp-8-Br-cAMPS (Fig.6*D,* Fig.7*A*). Rp-cAMPS is an inhibitor of both PKA and Epac, but it has a low affinity for Epac compared to 8-pCPT-2'-O-Me-cAMP (H. Rehmann and J. Bos, unpublished findings). The action of 8-pCPT-2'-O-Me-cAMP was dose-dependent over a concentration range of 10-100 μM (Fig.7*A*), and was not blocked by 10 μM of the PKA inhibitors H-89 or KT 5720 (Fig.7*A*). However, the action of 8-pCPT-2'-O-Me-cAMP was diminished by transfection of INS-1 cells with dominant negative pSRα Epac2 (Fig.7*A*). Dominant negative Epac2 does not bind cAMP because G114E and G422D amino acid substitutions have been introduced into the protein's two cAMP-binding domains (17).

PKA-independence of 8-pCPT-2'-O-Me-cAMP action- To examine the specificity with which 8-pCPT-2'-O-Me-cAMP differentiates between Epac and PKA, INS-1 cells were transfected with a plasmid in which expression of luciferase was placed under the control of multimerized cyclic AMP response elements (CRE-Luc). This reporter is activated by cAMP via a PKA signaling mechanism involving CREB (13-15). The activity of CRE-Luc was stimulated by 30-300 μM 8-CPT-cAMP (active at PKA and Epac), and was reduced by the PKA inhibitor H-89 (Fig.7*B*). However, 8-pCPT-2'-O-Me-cAMP failed to stimulate CRE-Luc (Fig.7*B*). Identical findings were obtained when evaluating the actions of 8-CPT-cAMP, H-89, and 8-pCPT-2'-O-Me-cAMP in HEK 293 cells transfected with CRE-Luc (data not shown). These observations demonstrate that when tested *in vitro* at a concentration of 30-300 μM, 8-pCPT-2'-O-Me-cAMP exhibits little or no efficacy as a stimulator of the cAMP, PKA, and CREB signaling pathways in INS-1 cells.

Ca^{2+} stores targeted by 8-pCPT-2'-O-Me-cAMP- GLP-1 or the GLP-1 receptor agonist exendin-4 (Ex-4) mobilizes Ca^{2+} from ryanodine-sensitive Ca^{2+} stores in INS-1 cells (18). In the present study, we found that CICR in response to 8-pCPT-2'-O-Me-cAMP was also blocked by ryanodine (Fig.8). However, it was recently reported that Epac mediates stimulatory actions of cAMP on IP_3-sensitive Ca^{2+} stores in HEK 293 cells (19,20). This action of cAMP is proposed to result from Epac-mediated activation of phospholipase C-epsilon (PLC-ε), with concomitant stimulation of inositol trisphosphate (IP_3) production (19,20). Therefore, Ca^{2+} mobilized by 8-pCPT-2'-O-Me-cAMP as a consequence of CICR in INS-1 cells might originate from Ca^{2+} stores regulated not only by ryanodine receptors (RYR) but also by inositol trisphosphate receptors (IP_3-R). INS-1 cells express muscarinic cholinergic receptors, and acetylcholine is a stimulus for inositol phosphate (IP) production (Table 1). However, a role for IP_3-R in Epac-mediated signal transduction in INS-1 cells appears unlikely because no stimulation of IP production was observed in INS-1 cells exposed to 8-pCPT-2'-O-Me-cAMP, GLP-1, or Ex-4 (Table 1).

DISCUSSION

8-pCPT-2'-O-Me-cAMP as a stimulator of β-cell stimulus-secretion coupling - Until now, no certain means by which to specifically activate Epac was available. Here we demonstrate that a newly developed Epac-selective cAMP analog (8-pCPT-2'-O-Me-cAMP) is a stimulator of CICR and exocytosis in human β-cells. 8-pCPT-2'-O-Me-cAMP is also demonstrated to stimulate CICR in an insulin-secreting cell line (INS-1), and this effect is PKA-independent because it is not blocked by H-89, KT 5720, or Rp-8-Br-cAMPS. Over expression of a dominant negative Epac2 abrogates CICR in response to 8-pCPT-2'-O-Me-cAMP, as expected because there exists in INS-1 cells an Epac2 signaling pathway critical to hormonal regulation of Ca^{2+} signaling (18). The specificity with which 8-pCPT-2'-O-Me-cAMP differentiates between PKA and Epac is emphasized by its failure to reproduce the action of 8-CPT-cAMP in an assay of CRE-Luc activity that is diagnostic of cAMP/PKA/CREB signal transduction. Therefore, 8-pCPT-2'-O-Me-cAMP is demonstrated to posses unique Epac-selective properties that should allow its wide spread use in assays of multiple cellular functions.

Implications for GLP-1 receptor signal transduction in β-cells- One difference between the findings of the present study and those of our previous report (18) is that H-89 and Rp-8-Br-cAMPS fail to block the action of 8-pCPT-2'-O-Me-cAMP, whereas both compounds exert inhibitory effects when examining the action of GLP-1 receptor agonist exendin-4 (18). These contrasting results are understandable if 8-pCPT-2'-O-Me-cAMP acts exclusively via Epac2, whereas exendin-4 acts not only via Epac2, but also PKA. It is also noteworthy that in some INS-1 cells a sustained increase of $[Ca^{2+}]_i$ is observed in response to 8-pCPT-2'-O-Me-cAMP, and it is preceded by CICR (c.f., Figs. 6D,8B). This biphasic response to 8-pCPT-2'-O-Me-cAMP is reminiscent of the action of GLP-1 in β-cells (8). GLP-1 is an inhibitor of ATP-sensitive K^+ channels (K-ATP), and by doing so

it produces β-cell depolarization, activation of Ca^{2+} influx, and a sustained increase of $[Ca^{2+}]_i$ (21,22). It will be of interest to ascertain if a similar inhibition of K-ATP is observed in response to 8-pCPT-2'-O-Me-cAMP acting as an Epac-selective modulator of K^+ channel function. In this regard, it is noteworthy that Epac contains not only Rap1 recognition motifs within its guanyl nucleotide exchange factor (GEF) catalytic domain, but also additional protein-protein interaction motifs within its DEP domain where homologies to *disheveled*, *Egl-10,* and pleckstrin are found. A physical association of Epac and the SUR1 subunit of K-ATP has been reported on the basis of a yeast two hybrid screen (17), so it is reasonable to speculate that the targets of Epac action may also include cell surface K-ATP channels.

Epac targets ryanodine receptor-regulated Ca^{2+} stores- Epac mediates stimulatory actions of cAMP on phospholipase C-ε in HEK 293 cells (19,20). The resultant increase of $[IP_3]$ serves as a stimulus for CICR mediated by the IP_3-R. However, we find that the Ca^{2+} mobilizing action of 8-pCPT-2'-O-Me-cAMP is unlikely to be a consequence of Epac-mediated IP_3 production. 8-pCPT-2'-O-Me-cAMP fails to increase levels of inositol phosphates in INS-1 cells loaded with ^{3}H-inositol. Instead, available evidence indicates an important role for ryanodine receptors (RYR) as targets of Epac action (8,18,23). Indeed, pretreatment of INS-1 cells with ryanodine blocks CICR in response to 8-pCPT-2'-O-Me-cAMP. Furthermore, it was previously reported that treatment of INS-1 cells with the IP_3-R inhibitor *Xestospongin* C fails to block CICR in response to forskolin (18). Since our methods of analysis were restricted to use of a dominant negative Epac2, no conclusion can yet be reached concerning what role Eapc1 may play in β-cell Ca^{2+} signaling. However, 8-pCPT-2'-O-Me-cAMP is an activator of Epac1 (4), and in the present study it failed to stimulate inositol phosphate production. Although these findings argue against a role for the IP_3 receptor as a target of Epac1 and Epac2 action in β-cells, additional studies are necessary in order to reach a firm conclusion.

Coupling of Epac to endoplasmic reticulum Ca^{2+} stores-

Previous studies of INS-1 cells demonstrated that cAMP-elevating agents mobilize Ca^{2+} from thapsigargin-sensitive Ca^{2+} stores (18). These Ca^{2+} stores are most likely located in the endoplasmic reticulum (ER) where the SERCA Ca^{2+} ATPase targeted by thapsigargin is found. One possible effector that links Epac signaling to these Ca^{2+} stores is Rap1, a small molecular weight G protein previously reported to form direct protein-protein interactions with SERCA (24). In addition, an Epac/Rap1 signaling complex in the ER might influence Ca^{2+} signaling by modulating RYR gating properties, possibly through direct interactions with the channel. Such an effect might synergize with PKA-mediated sensitization of RYR, thereby facilitating Ca^{2+} release from the ER (25). In this regard, HEK 293 cells over expressing the GLP-1-R exhibit ryanodine-sensitive CICR in response to GLP-1, and this action correlates with the ability of GLP-1 to stimulate cAMP production (26). Therefore, the targeting of RYR by GLP-1, whether direct or indirect, is a signaling mechanism not restricted to β-cells.

Functional coupling of CICR to exocytosis- Here we also demonstrate that 8-pCPT-2'-O-Me-cAMP stimulates Ca^{2+}-dependent exocytosis in human β-cells. Exocytosis is observed to be time-locked to the increase of $[Ca^{2+}]_i$ generated by CICR, and indeed, no exocytosis is observed in the absence of CICR. It appears, therefore, that an increase of $[Ca^{2+}]_i$ is a necessary and not simply permissive stimulus for initiation of exocytosis. Of course this conclusion does not preclude additional Epac-mediated signaling events important to secretion. For example, the interaction of Epac with Rim2, an insulin granule-associated protein, might play an important role in conferring stimulatory effects of cAMP on exocytosis in β-cells (17,27-29). Despite this caveat, it is clear that the mobilization of Ca^{2+} by cAMP is a highly significant feature of β-cell stimulus-secretion coupling. Indeed, we recently reported that CICR serves to amplify exocytosis in INS-1 cells (12).

Conclusion- The present findings are noteworthy because we demonstrate a functional coupling of Epac-mediated CICR to exocytosis in human β-cells. This coupling is revealed through the use of a newly developed Epac-selective cAMP analog. The findings are of medical importance because they shed light on the blood glucose lowering properties of an insulinotropic hormone (GLP-1) currently under investigation for use in the treatment of type-2 diabetes mellitus (30,31). Multiple PKA-independent actions of GLP-1 have been reported in β-cells, and these actions include effects of GLP-1 on Ca^{2+} signaling (18,32), K-ATP (33), insulin-granule associated Rim2 proteins (17,27) and insulin gene expression (13,15). Findings presented here demonstrate that 8-pCPT-2'-O-Me-cAMP is likely to serve as a powerful pharmacological tool for assessment of Epac-mediated signaling events that underlie such poorly understood effects of GLP-1.

Acknowledgements- G.G. Holz acknowledges the support of the National Institutes of Health (R01-DK45817, R01-DK52166), the American Diabetes Association (Research Grant Award), and the Marine Biological Laboratory, Woods Hole, MA (Research Fellowship). M.B. Wheeler is supported by operating (MOP12898) and salary grants from the Canadian Institutes of Health Research (CIHR). J.W. Joseph is supported by a CIHR doctoral student award. pSRα Epac2 plasmids were the gift of Dr. S. Seino. GGH acknowledges the contribution of human islets from JDRFI-funded islet transplantation centers located at the University of Minnesota (Dr. B.J. Hering), Washington University (Dr. B.J. Olack), and the University of Miami (Dr. C. Ricordi).

Figure Legends

Figure 1. ***Rat insulin II gene promoter-directed expression of EYFP.*** Stable transfection of INS-1 cells (top two panels) was achieved by use of RIP2-EYFP allowing antibiotic resistance selection using G418. Expression of EYFP in single human β-cells (bottom two panels) was achieved by infection of primary islet cell cultures with adenovirus incorporating RIP2-EYFP. In human β-cells the subcellular localization of EYFP was either cytosolic (bottom, left) or nuclear (bottom, right). Calibration bars: *A*, 20 μm, *B* 10 μm, *C* and *D,* 5 μm.

Figure 2. ***β-cell specific expression of EYFP conferred by RIP2***. Left panel, confocal microscopy demonstrates co-localization of EYFP and insulin-like immunoreactivity in a rat islet infected with adenovirus incorporating RIP2-EYFP. *A*, bright field image of a rat islet; *B*, detection of EYFP in this islet; *C,* insulin-like immunoreactivity in this islet; *D*, image overlap of *B* and *C* demonstrating co-expression of insulin and EYFP (orange) in β-cells. Right panel, glucagon but not EYFP is expressed in rat α-cells infected with RIP2-EYFP. *E*, bright field image of an islet; *F*, detection of EYFP in this islet; *G,* glucagon-like immunoreactivity in this islet; *H*, image overlap of *F* and *G* demonstrating that EYFP is not expressed in α-cells.

Figure 3. ***Expression of EYFP in human β-cells correlates with sulfonylurea-sensitivity***. A cluster of three human islet cells was evaluated for expression of EYFP under conditions of fura-2 loading. The cell labeled #1 (top panel) exhibited an increase of $[Ca^{2+}]_i$ (bottom panel) in response to a 10 sec application of 100 nM glyburide applied to the entire cluster of cells. This same cell contained EYFP (bottom panel inset; note that the boundary surrounding the cluster of cells is indicated by a white outline). The remaining two cells of the cluster did not contain EYFP and failed to respond to glyburide. Identical findings were obtained in a total of 5 separate experiments.

Figure 4. ***Human β-cells are sensitive to 8-pCPT-2'-O-Me-cAMP***. *A*, a single EYFP-positive cell was imaged for fura-2 (A*1*) and 8-pCPT-2'-O-Me-cAMP (50 μM) was applied via a micropipette for 10 sec. CICR was measured as a transient increase of $[Ca^{2+}]_i$ (A*2*). The β-cell phenotype was confirmed by demonstrating the ability of this cell to respond to a 10 sec application of glyburide (A*2*; Glyb., 100 nM). Identical findings were obtained in a total of 10 human β-cells tested. *B*, CICR in response to 8-pCPT-2'-O-Me-cAMP was inhibited by treatment of a human β-cell with ryanodine. Arrows indicate a 10 sec application of 100 μM 8-pCPT-2'-O-Me-cAMP with or without 10 μM ryanodine (Ryan.). Horizontal bar indicates the duration of pretreatment with 10 μM ryanodine applied directly to the solution bathing the cell. Identical findings were obtained in a total of 4 cells tested.

Figure 5. ***8-pCPT-2'-O-Me-cAMP as a stimulus for CICR and exocytosis.*** A human β-cell was loaded with fura-2 and 5-HT for simultaneous measurements of $[Ca^{2+}]_i$ and exocytosis. Application of 8-pCPT-2'-O-Me-cAMP (100 μM, 10 sec) produced CICR (*A1*) and exocytosis of 5-HT (*A2*), as depicted on a compressed time scale. When viewed on an expanded time scale, the quantal nature of the individual secretory events (upward amperometric current spikes due to oxidation of 5-HT) was revealed (*A3*;*A4*). Identical findings were obtained in a total of 10 human β-cells tested.

Figure 6. ***8-pCPT-2'-O-Me-cAMP as a stimulus for CICR in INS-1 cells.*** INS-1 cells loaded with fura-2 exhibited a transient increase of $[Ca^{2+}]_i$ in response to 50 μM 8-pCPT-2'-O-Me-cAMP (*A*). The action of 8-pCPT-2'-O-Me-cAMP was mimicked by 10 μM forskolin (*B*, forsk.) and by 1 mM 8-Br-cAMP (*C*). Bath application of 300 μM Rp-8-Br-cAMPS 10 min prior to and during application of the test substance failed to block the action of 50 μM 8-pCPT-2'-O-Me-cAMP (*D*). Arrows indicate a 10 sec application of each test substance. To assure the reproducibility of these findings, the action of each test substance was confirmed in a minimum of 4 separate experiments using 12 or more INS-1 cells.

Figure 7. ***Pharmacological properties of 8-pCPT-2'-O-Me-cAMP.*** *A,* a population study of INS-1 cells was performed and the percentage of cells exhibiting CICR in response to 8-pCPT-2'-O-Me-cAMP was determined. The action of 100 μM 8-pCPT-2'-O-Me-cAMP was dose-dependent (* indicates statistical significance < 0.001 relative to 10 μM) and was not blocked by H-89 (10 μM), KT 5720 (10 μM), or Rp-8-Br-cAMPS (300 μM). Transfection of INS-1 cells with dominant negative Epac2 blocked the action of 8-pCPT-2'-O-Me-cAMP (100 μM), whereas transfection with wild-type (WT) Epac2 did not (* indicates statistical significance < 0.001 relative to WT Epac). Transfected cells were identified by use of RIP2-EYFP as described previously (18) *B,* 8-pCPT-2'-O-Me-cAMP failed to stimulate luciferase activity in INS-1 cells transfected with CRE-Luc. Application of the structurally-related PKA activator 8-CPT-cAMP produced a dose-dependent stimulation of CRE-Luc, and the action of 8-CPT-cAMP was reduced by the PKA inhibitor H-89 (10 μM). (** indicates statistical significance < 0.005 relative to 30, 100, or 300 μM 8-CPT-cAMP in the absence of H-89). This experiment was repeated twice, and the effect of each concentration of test substance was evaluated in triplicate.

Figure 8. ***Ryanodine-sensitivity of 8-pCPT-2'-O-Me-cAMP-induced CICR.*** Ryanodine (10 μM) was applied to INS-1 cells by use of a micropipette. A second micropipette was then positioned adjacent to the ryanodine pretreated cell in order to deliver a test solution containing 8-pCPT-2'-O-Me-cAMP (100 μM) and ryanodine (10 μM). In 2 of 10 cells tested, ryanodine produced a reversible block of CICR (*A*), whereas in 8 of 10 cells no recovery from the inhibitory action of ryanodine was observed (*B*). Arrows indicate a 10 sec application of test substances. The duration of ryanodine pretreatment is indicated by a horizontal bar. Similar findings were obtained using a 1 μM concentration of ryanodine (data not shown).

REFERENCES

1. de Rooij, J., Zwartkruis, F.J.T., Verheijen, M.H.G., Cool, R.H., Nijman, S.M.B., Wittinghofers, A., and Bos, J.L. (1998) *Nature* **396,** 474-477.
2. Kawasaki, H., Springett, G.M., Mochizuki, N., Toki, S., Nakaya, M., Matsuda, M., Housman, D.E. and Graybiel, A.M. (1998) *Science* **282,** 2275-2279.
3. Schwede, F., Maronde, E., Genieser, H.-G. and Jastorff, B. (2000) *Pharmacol. Ther.* **87,** 199 - 226.
4. Enserink, J.M., Christensen, A.E., de Rooij, J., Triest, M.V., Schwede, F., Genieser, H.G., Døskeland, S.O., Blank, J.L., and Bos, J.L. (2002) *Nat. Cell Biol.* **4,** 901-906.
5. Asfari, M., Janjic, D., Meda, P., Li, G., Halban, P. A. and Wollheim, C.B. (1992) *Endocrinology* **130,** 167-178.
6. Chan, C.B., MacDonald, P.E., Saleh, M.C., Johns, D.C., Marban, E., Wheeler, M.B. (1999) *Diabetes* **48,** 1482-1486.
7. Grynkiewicz, G., Poenie, M. and Tsien, R. Y. (1985) *J. Biol. Chem.* **260,** 3440-3450.
8. Holz, G. G., Leech, C. A., Heller, R. S., Castonguay, M. and Habener, J. F. (1999) *J. Biol. Chem.* **274,** 14147-14156.
9. Ekholm, R., Ericson, L. E., and Lundquist, I. (1971) *Diabetologia* **7,** 339-348.
10. Aspinwall, C. A., Huang, L., Lakey, J. R. and Kennedy, R. T. (1999) *Analytical Chemistry* **71,** 5551-5556.
11. Zawalich, W. S., Tesz, G. J., and Zawalich, K. C. (2001) *J. Biol. Chem.* **276,** 37120-37123.
12. Kang, G. and Holz, G.G. (in press) *J. Physiol. (Lond.)*
13. Skoglund, G., Hussain, M. A. and Holz, G. G. (2000) *Diabetes* **49,** 1156-1164.
14. Chepurny, O.G. and Holz, G.G. (2002) *Cell Tissue Res.* **307,** 191-201.
15. Chepurny, O.G., Hussain, M.A. and Holz, G.G. (2002) *Endocrinology* **143,** 2303-2313.
16. Koreh, K. and Monaco, M.E. (1986) *J. Biol. Chem.* **261,** 88-91.

17. Ozaki, N., Shibasaki, T., Kashima, Y., Miki, T., Takahashi, K., Ueno, H., Sunaga, Y., Yano, H., Matsuura, Y., Iwanaga, T., Takai, Y. and Seino, S. (2000) *Nat. Cell. Biol.* **11,** 805-811.
18. Kang, G., Chepurny, O.G., Holz, G.G. (2001) *J. Physiol.(Lond.)* **536,** 375-385.
19. Schmidt, M., Evellin, S., Weernink,, P.A., von Dorp, F., Rehmann, H., Lomasney, J.W. and Jakobs, K.H. (2001) *Nat. Cell. Biol.* **3,** 1020-1024.
20. Evellin, S., Nolte, J., Tysack, K., vom Dorp, F., Thiel, M., Weernink,, P.A., Jakobs, K.H., Webb, E.J., Lomasney, J.W. and Schmidt, M. (2002) *J. Biol. Chem.* **277,** 16805-16813.
21. Holz, G.G. and Habener, J.F. (1992) *Trends Biochem. Sci.* **17,** 388-393.
22. Holz, G.G., Kuhtreiber, W.M., Habener, J.F. (1993) *Nature* **361,** 362-365.
23. Islam, M.S. (2002) *Diabetes* **51,** 1299-1309.
24. Lacabaratz-Porret, C., Corvazier, E., Kovacs, T., Bobe, R. and Bredoux, R. (1998) *Biochem. Journal* **332,** 173-181.
25. Marx, S.O., Reiken, S., Hisamatsu, Y., Jayaraman, T., Burkhoff, D., Rosemblit, N. and Marks A.R. (2000) *Cell* **101,** 365-376.
26. Gromada, J., Rorsman, P., Dissing, S. and Wulff, B.S. (1995) *FEBS Lett.* **373,** 182-186.
27. Kashima, Y., Miki, T., Shibasaki, T., Ozaki, N., Miyazaki, M., Yano, H. and Seino, S. (2001) *J. Biol. Chem.* 276, 46046-46053.
28. Renström, E., Eliasson, L. and Rorsman, P. (1997) *J. Physiol. (Lond.)* **502,** 105-118.
29. Leech, C.A., Holz, G.G., Chepurny, O. and Habener, J.F. (2000) *Biochem. Biophys. Res. Comm.* **278,** 44-47.
30. Drucker, D.J. (1998) *Diabetes* **47,** 159-169.
31. Kieffer T.J. and Habener J.F. (1999) *Endocrine Review* **20,** 876-913.
32. Bode, H.P., Moormann, B., Dabew, R. and Göke B. (1999) *Endocrinology* **140,** 3919-3927.
33. Suga, S., Kanno, T., Ogawa, Y., Takeo, T., Kamimura, N. and Wakui, M. (2000) *Pflügers Arch.* **440,** 566-572.

Table 1.

	Inositol Phosphate Accumulation (cpm/well)	p value	n
Addition			
None	3144 +/- 460		8
Acetylcholine (100μM)	5416 +/- 456	p<0.0005	4
8-CPT-2-Me-cAMP (30μM)	2508 +/- 120	NS	4
8-CPT-2-Me-cAMP (100μM)	3048 +/- 636	NS	4
8-CPT-2-Me-cAMP (300μM)	3024 +/- 368	NS	4
Exendin-4 (100 nM)	3324 +/- 220	NS	4
GLP-1 (100 nM)	2656 +/- 220	NS	4

Legend: Inositol phosphate production in INS-1 cells was stimulated by acetylcholine but not 8-CPT-2-Me-cAMP, exendin-4, or GLP-1. Incorporation of tritiated inositol into total cellular phosphoinositides prior to stimulation was 7550 +/- 1398 cpm per well. Abbreviations: NS, not significant.

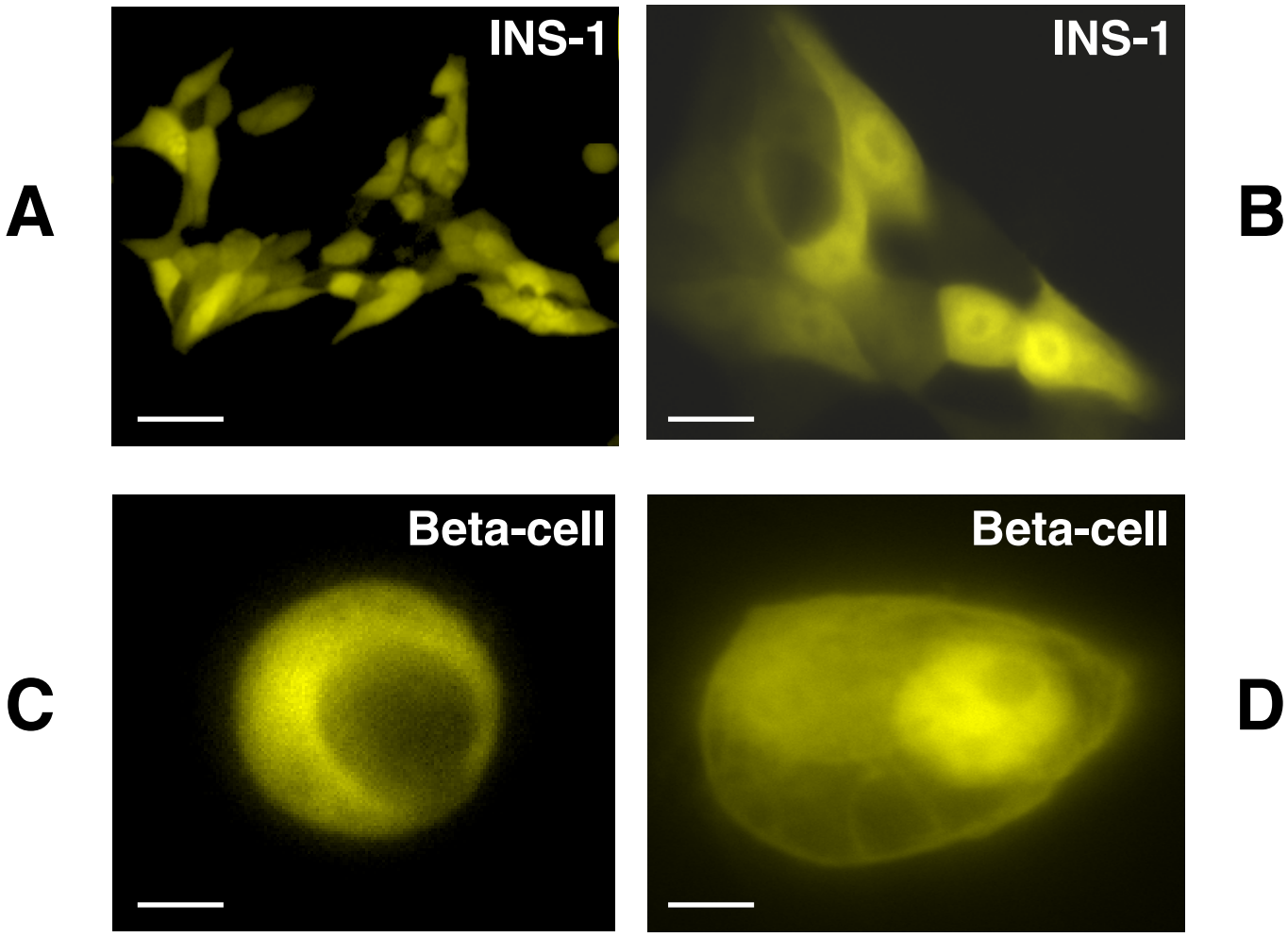
A
INS-1
B
INS-1
C
Beta-cell
D
Beta-cell

Rat Islet

Co-Expression Of EYFP And Insulin

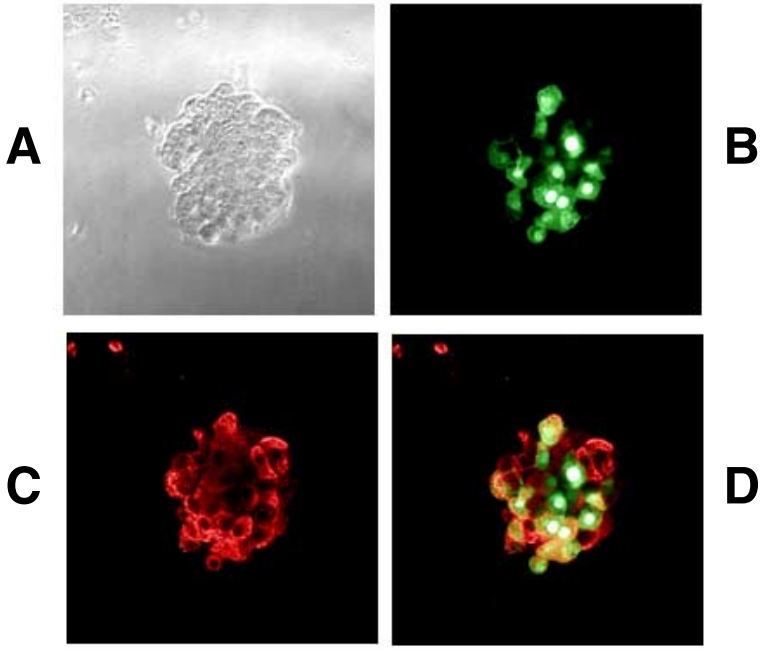

Rat Islet

EYFP And Glucagon Do Not Co-Localize

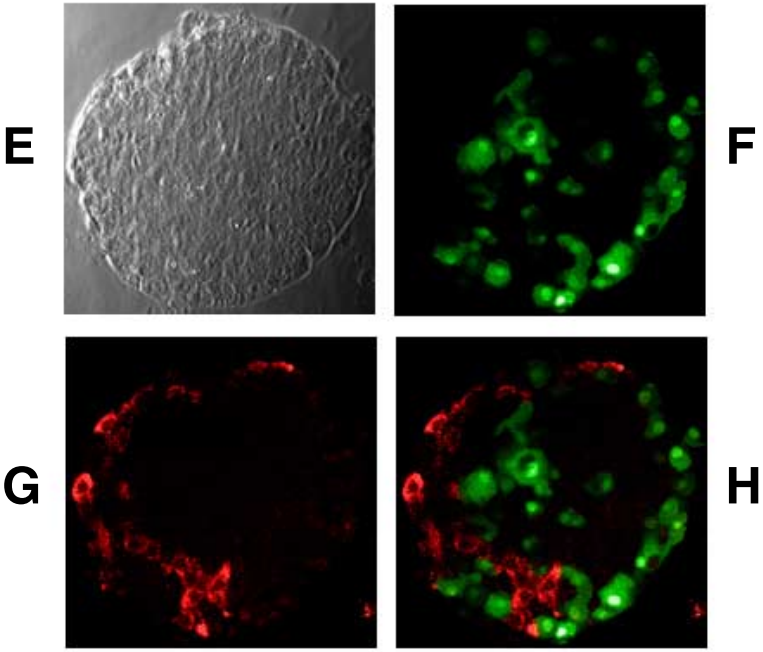

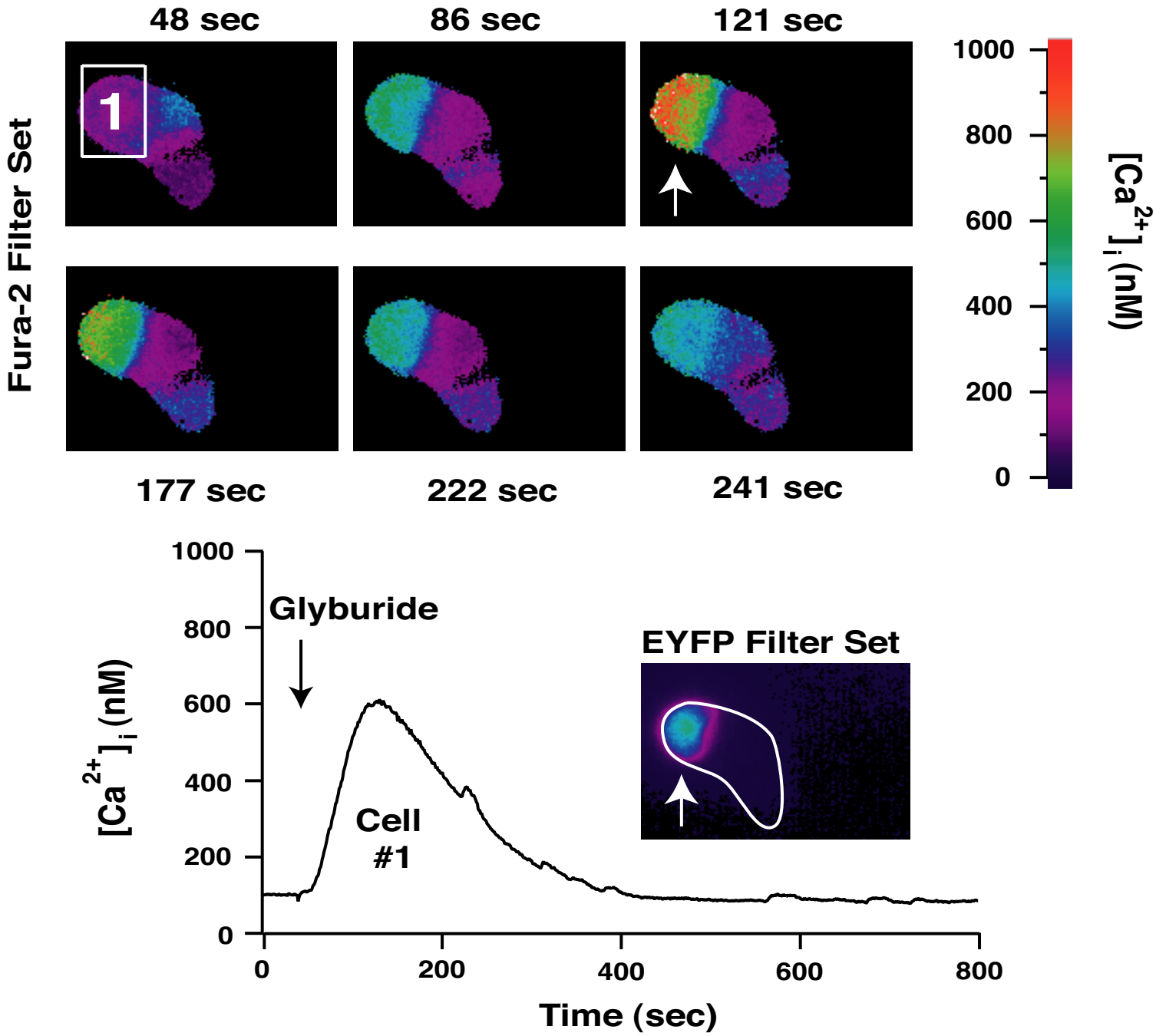
48 sec
86 sec
121 sec
Fura-2 Filter Set
1
177 sec
222 sec
241 sec
1000
800
600
400
200
0
[Ca2+]i (nM)
Glyburide
EYFP Filter Set
Cell
#1
[Ca2+]i (nM)
0
200
400
600
800
Time (sec)

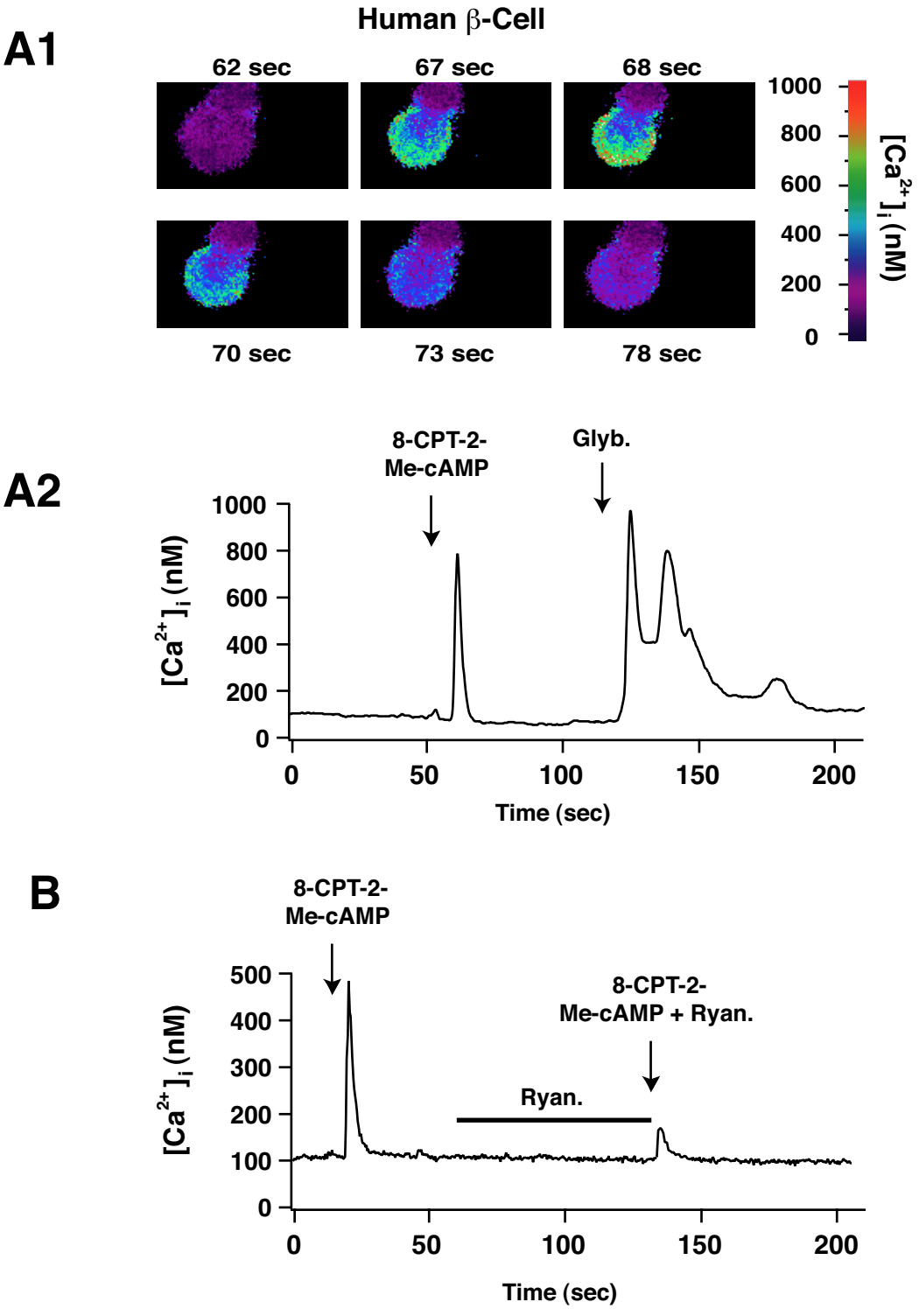
A1
Human β-Cell
62 sec
67 sec
68 sec
70 sec
73 sec
78 sec
1000
800
600
400
200
0
[Ca2+]i (nM)
A2
8-CPT-2-
Me-cAMP
Glyb.
[Ca2+]i (nM)
Time (sec)
B
8-CPT-2-
Me-cAMP
8-CPT-2-
Me-cAMP + Ryan.
Ryan.
[Ca2+]i (nM)
Time (sec)

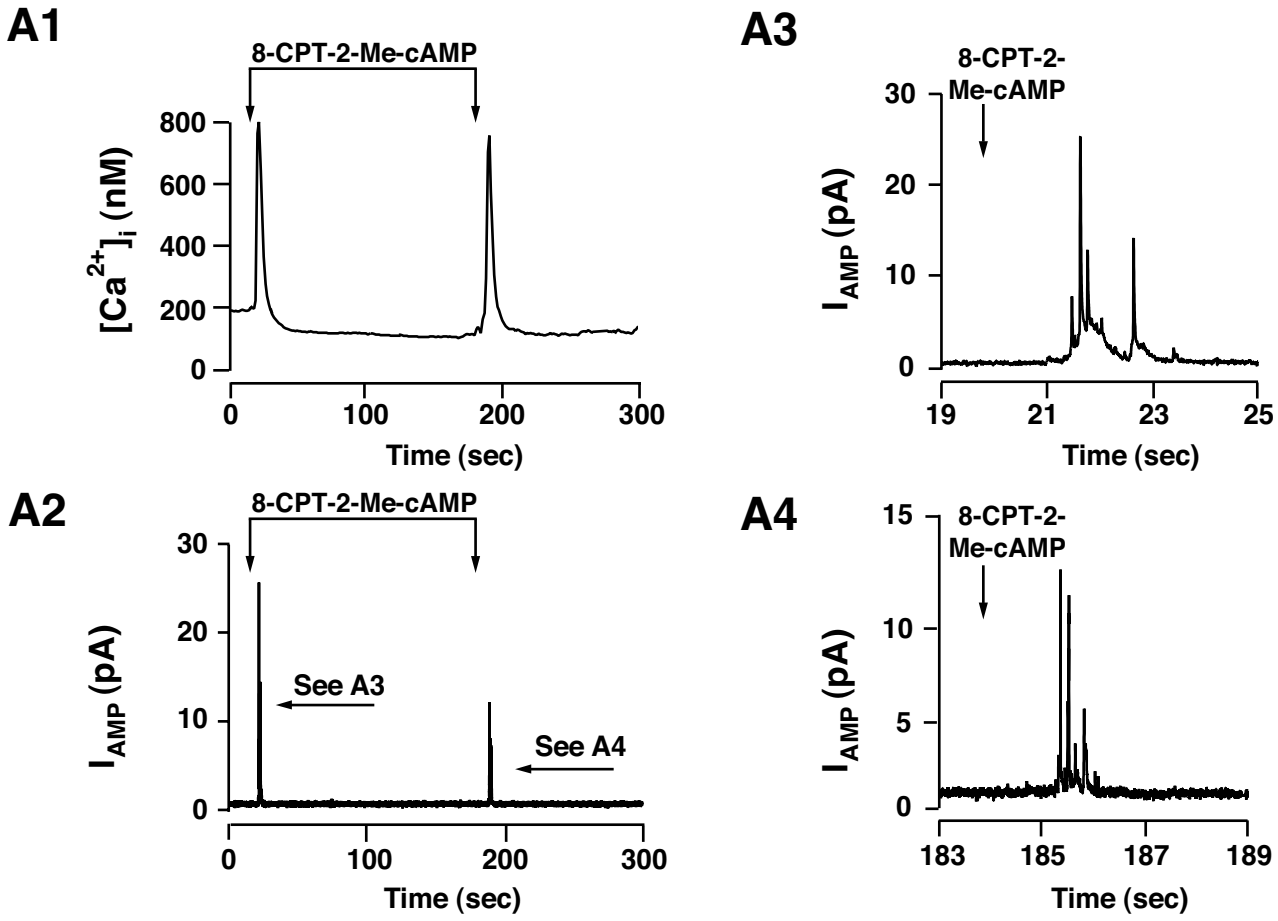
A1
8-CPT-2-Me-cAMP
800
600
400
200
0
[Ca2+]i (nM)
0
100
200
300
Time (sec)
A2
8-CPT-2-Me-cAMP
30
20
10
0
IAMP (pA)
See A3
See A4
0
100
200
300
Time (sec)
A3
8-CPT-2-
Me-cAMP
30
20
10
0
IAMP (pA)
19
21
23
25
Time (sec)
A4
8-CPT-2-
Me-cAMP
15
10
5
0
IAMP (pA)
183
185
187
189
Time (sec)

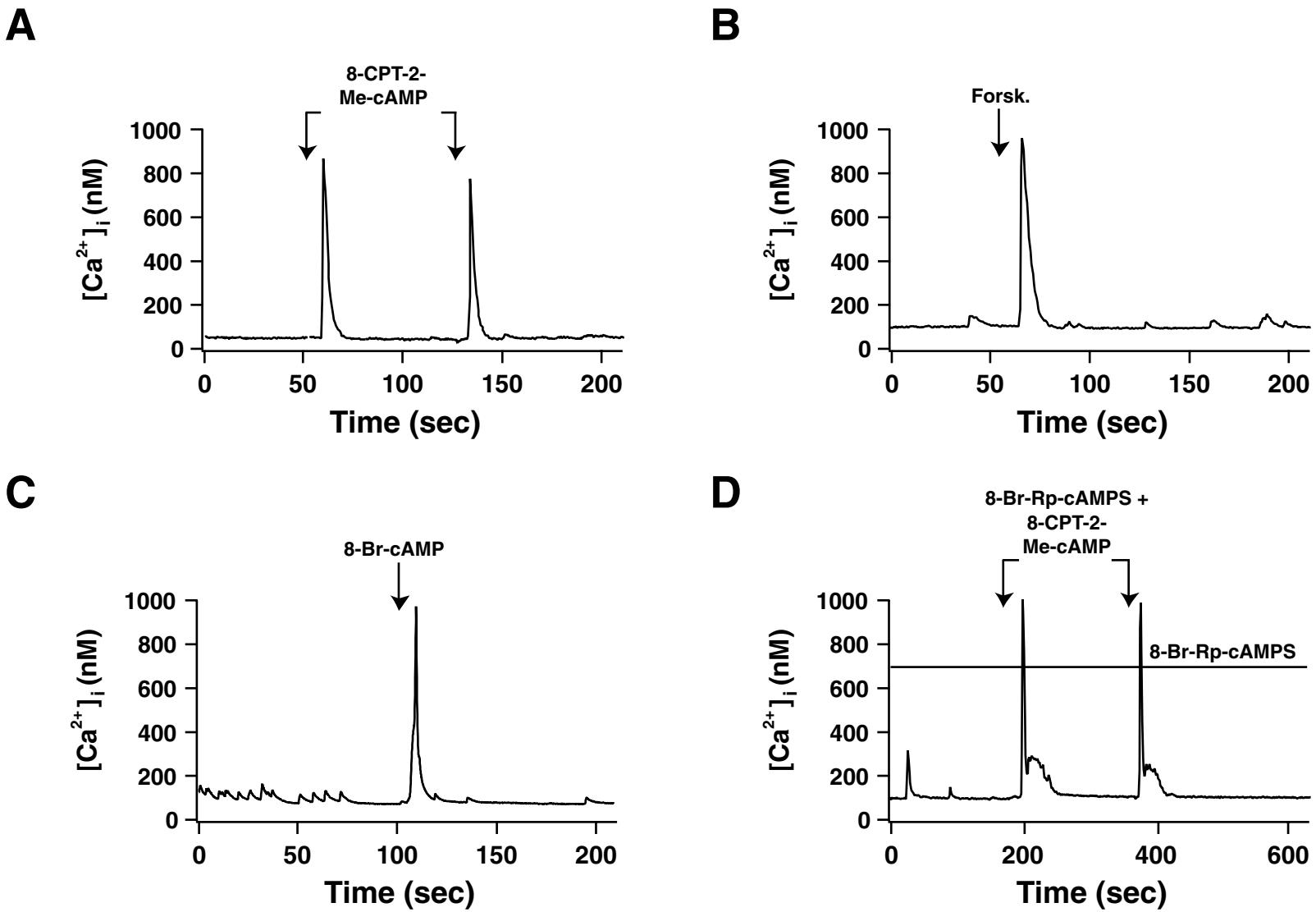
A
8-CPT-2-
Me-cAMP
[Ca2+]i (nM)
1000
800
600
400
200
0
0
50
100
150
200
Time (sec)
B
Forsk.
[Ca2+]i (nM)
1000
800
600
400
200
0
0
50
100
150
200
Time (sec)
C
8-Br-cAMP
[Ca2+]i (nM)
1000
800
600
400
200
0
0
50
100
150
200
Time (sec)
D
8-Br-Rp-cAMPS +
8-CPT-2-
Me-cAMP
8-Br-Rp-cAMPS
[Ca2+]i (nM)
1000
800
600
400
200
0
0
200
400
600
Time (sec)

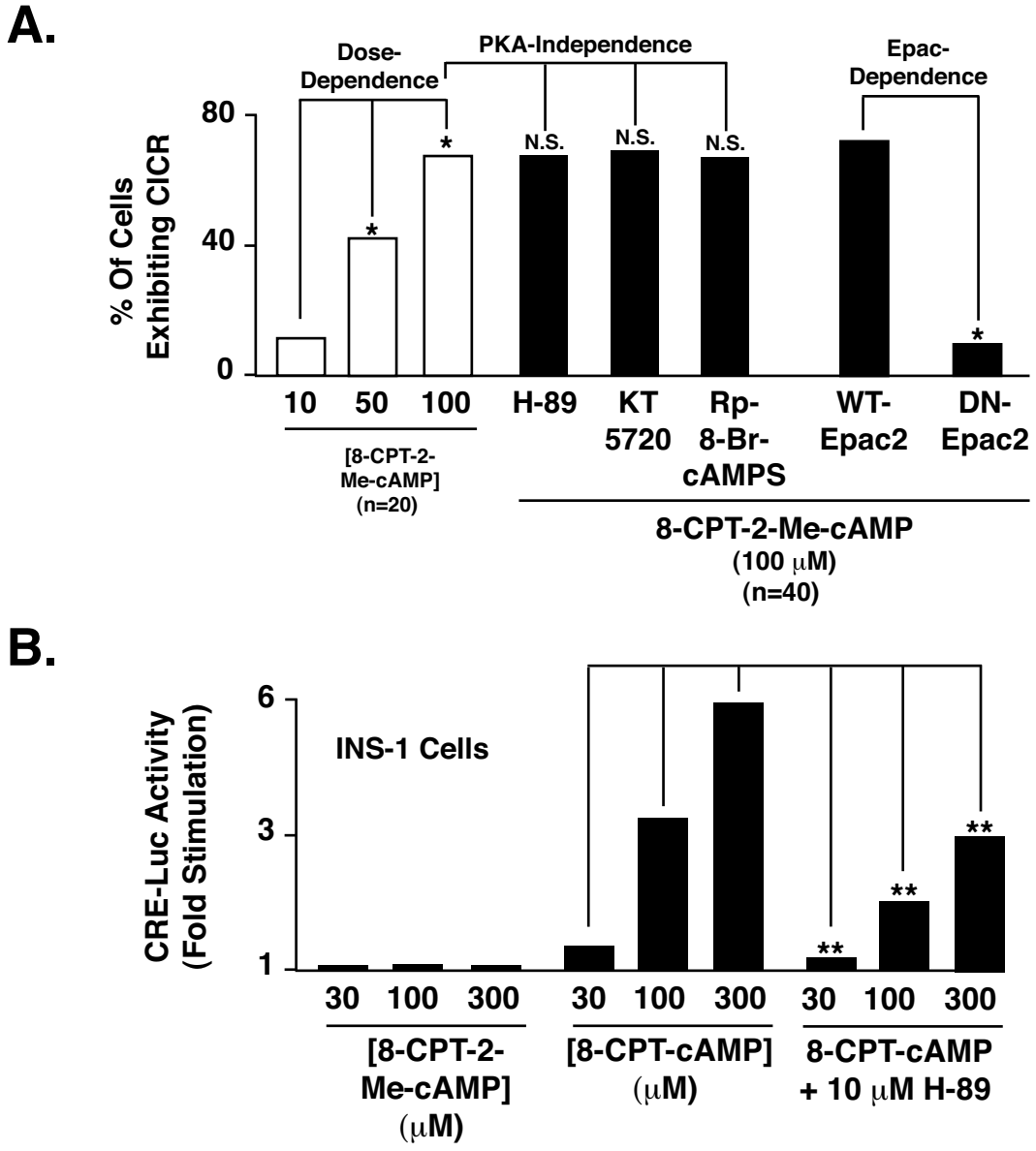
A.
Dose-Dependence
PKA-Independence
Epac-Dependence
% Of Cells Exhibiting CICR
80
40
0
*
*
N.S.
N.S.
N.S.
*
10
50
100
H-89
KT 5720
Rp-8-Br-cAMPS
WT-Epac2
DN-Epac2
[8-CPT-2-Me-cAMP] (n=20)
8-CPT-2-Me-cAMP (100 μM) (n=40)
B.
CRE-Luc Activity (Fold Stimulation)
INS-1 Cells
6
3
1
**
**
**
30
100
300
30
100
300
30
100
300
[8-CPT-2-Me-cAMP] (μM)
[8-CPT-cAMP] (μM)
8-CPT-cAMP + 10 μM H-89

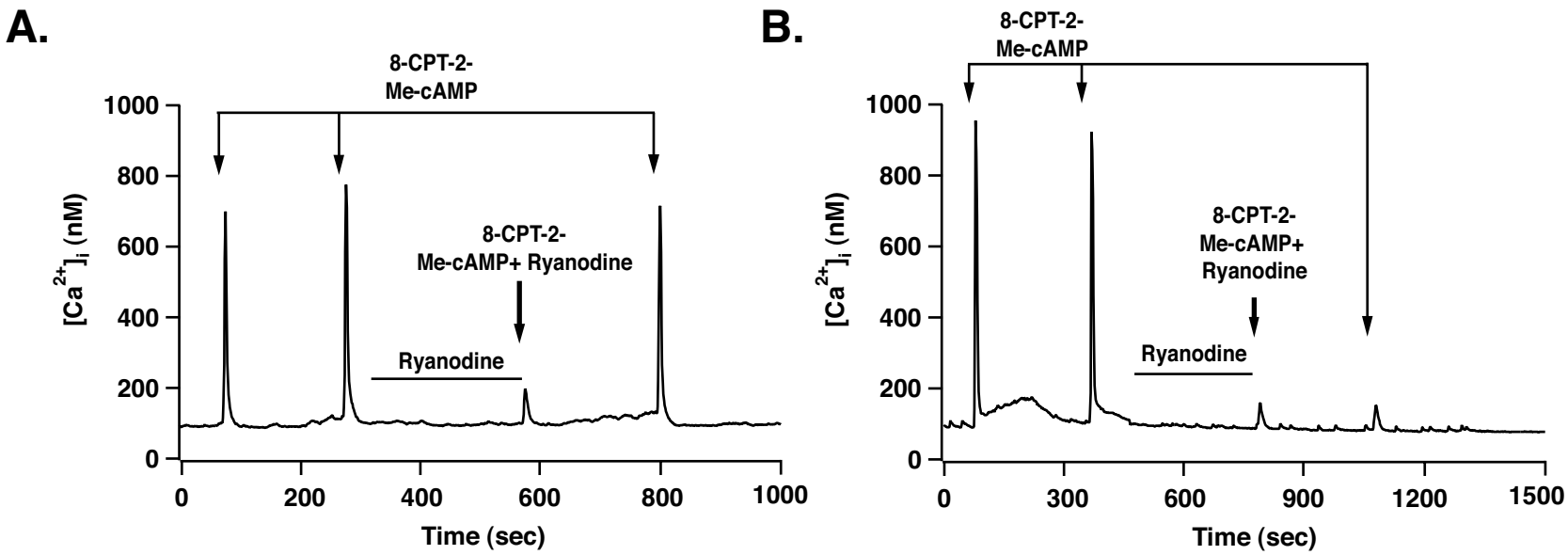
A.
8-CPT-2-
Me-cAMP
8-CPT-2-
Me-cAMP+ Ryanodine
Ryanodine
[Ca2+]i (nM)
1000
800
600
400
200
0
0
200
400
600
800
1000
Time (sec)
B.
8-CPT-2-
Me-cAMP
8-CPT-2-
Me-cAMP+
Ryanodine
Ryanodine
[Ca2+]i (nM)
1000
800
600
400
200
0
0
300
600
900
1200
1500
Time (sec)

Table 1.

	Inositol Phosphate Accumulation (cpm/well)	p value	n
Addition			
None	3144 +/- 460		8
Acetylcholine (100μM)	5416 +/- 456	p<0.0005	4
8-CPT-2-Me-cAMP (30μM)	2508 +/- 120	NS	4
8-CPT-2-Me-cAMP (100μM)	3048 +/- 636	NS	4
8-CPT-2-Me-cAMP (300μM)	3024 +/- 368	NS	4
Exendin-4 (100 nM)	3324 +/- 220	NS	4
GLP-1 (100 nM)	2656 +/- 220	NS	4

Legend: Inositol phosphate production in INS-1 cells was stimulated by acetylcholine but not 8-CPT-2-Me-cAMP, exendin-4, or GLP-1. Incorporation of tritiated inositol into total cellular phosphoinositides prior to stimulation was 7550 +/- 1398 cpm per well. Abbreviations: NS, not significant.